

## Supporting Information

### Nitrogen-doped biomass carbon fibers with surface encapsulated Co nanoparticles for electrocatalytic overall water-splitting

Shihuan Hong,<sup>a</sup> Ning Song,<sup>a</sup> Jingxue Sun,<sup>b</sup> Gang Chen,<sup>b</sup> Hongjun Dong<sup>a</sup> and Chunmei Li<sup>\*a</sup>

<sup>a</sup>*Institute of Green Chemistry and Chemical Technology, School of Chemistry and Chemical Engineering, Jiangsu University, Zhenjiang 212013, PR China.*

<sup>b</sup>*MIIT Key Laboratory of Critical Materials Technology for New Energy Conversion and Storage, School of Chemistry and Chemical Engineering, Harbin Institute of Technology, 150001, PR China.*

#### 1. Experimental section

**Chemicals.** Platinum on carbon (Pt/C, 5% wt %, AR), ruthenium (IV) oxide (RuO<sub>2</sub>, 99.9%, AR) was purchased from Shanghai Macklin Biochemical Co., LTD. 2,2'-Bipyridyl (C<sub>10</sub>H<sub>8</sub>N<sub>2</sub>, 99%, AR), nickel chloride hexahydrate (NiCl<sub>2</sub>·6H<sub>2</sub>O, 98%, AR), potassium hydroxide (KOH, 99%, AR), sodium chlorite (NaClO<sub>2</sub>, 80%, AR) were purchased from Aladdin Chemical Reagents Co., LTD. Iron(II) chloride tetrahydrate (FeCl<sub>2</sub>·4H<sub>2</sub>O, 98%, AR), cobalt(II) nitrate hexahydrate (Co(NO<sub>3</sub>)<sub>2</sub>·6H<sub>2</sub>O, 98.5%, AR) were purchased from Sinopharm Chemical Reagent Co., Ltd. Nafion (5 wt %, AR) were purchased from Alfa Aesar. Cotton fibre was purchased from a farm in Changji City, Xinjiang Province, China. Deionized (DI) water was employed as solvent.

**Pretreatment of cotton.** Add the cotton fibers to the NaClO<sub>2</sub> (1 wt%) solution and magnetically stir for 10 minutes. The resulting suspension was refluxed at 120 °C for 4 hours to remove the wax protective layer on the surface. After filtration, it was washed several times with distilled water and dried at 60 °C overnight to obtain treated cotton fibers.

**Synthesis of the samples.** Firstly, 6.7 mmol Co (NO<sub>3</sub>)<sub>2</sub>·6H<sub>2</sub>O was dissolved in 10 ml absolute ethanol. Then, the above metal ion solution was slowly dropped into another 20ml of anhydrous ethanol solution containing 4mmol 2,2'-bipyridine and stirred under ambient conditions for 10 min. After that, 0.9g NaClO<sub>2</sub> treated cotton was put into 20ml mixed solution until the cotton absorbed all the solutions and dried at 60 °C. Then, the cotton was heated to 800 °C in a tubular furnace at a heating rate of 5 °C min<sup>-1</sup> and kept in a high purity argon gas stream for 4 hours. After calcination, the sample was stirred with 1wt% HCl for 3 days, washed with ethanol and deionized water 3 times, and finally dried at 60°C overnight to obtain the target product Co/N-BCFs. For comparison, Fe/N-BCFs and Ni/N-BCFs are prepared by the same method, adding the same molar mass of FeCl<sub>2</sub>·4H<sub>2</sub>O and NiCl<sub>2</sub>·6H<sub>2</sub>O instead of Co (NO<sub>3</sub>)<sub>2</sub>·6H<sub>2</sub>O. BCFs samples were prepared from NaClO<sub>2</sub> treated cotton in a tubular furnace at 800 °C for 4 h under an argon atmosphere with a temperature ramp of 5 °C min<sup>-1</sup>.

**Preparation the working electrode.** Typically, the ink was prepared by dispersing 5 mg of samples into 1ml mixture containing 960  $\mu\text{L}$  ethanol and 40  $\mu\text{L}$  Nafion (5 wt %) with an ultrasonic treatment for 30 min. Then, as-made ink of all the catalysts was dropped onto carbon paper ( $0.25 \times 0.25 \text{ cm}^2$ ) to afford a loading density of  $2.4 \text{ mg cm}^{-2}$ . After drying, the working electrodes were obtained. Electrochemical tests were carried out by using a VERSTAT-3 (Princeton Applied Research, America) electrochemical workstation with a conventional three-electrode system at room temperature, in which sample coated carbon paper electrode, the Hg/HgO electrode and platinum sheet served as the working, reference, and counter electrode, respectively. 1 M KOH solution was used as the electrolyte.

**Materials characterization.** X-ray diffraction (XRD) was recorded by a D/MAX-2500 diffractometer (Rigaku, Japan) with a Cu K $\alpha$  radiation source from  $10\text{--}80^\circ$ . Scanning electron microscopy (SEM) images were analyzed by JSM-7800F. Transmission electron microscopy (TEM) images were conducted on JEM-2800 electron microscope with an accelerating voltage of 200 kV. In addition, the chemical state of the sample was studied by the X-ray photoelectron spectroscopy (XPS) (Thermo Scientific K-Alpha), All XPS spectra were corrected using the C 1s line at 284.6 eV. Curve fitting and background subtraction were accomplished. Raman spectra were recorded on a Thermo Fisher DXR instrument with an Ar laser source of 532 nm in a macroscopic configuration. The Brunauer-EmmettTeller (BET) specific surface area and average pore diameter distribution were recorded by using a Micromeritics TriStar II3020 instrument. The ICP measurement was performed on Shimadzu ICPE-9820.

**Electrochemical measurements.** All electrochemical properties were collected using a three-electrode electrochemical system at room temperature. The electrocatalytic HER, OER and full water splitting activity were characterized in 1M KOH with a scan rate of  $5 \text{ mV s}^{-1}$ , and the electropotential for water oxidation was evaluated at  $10 \text{ mA cm}^{-2}$  current density ( $E_{j=10}$ ). Furthermore, the HER and OER potentials were converted to standard reversible hydrogen electrode (RHE) scale according to the equation:  $E \text{ (vs. RHE)} = E \text{ (vs. Hg/HgO)} + 0.059 \cdot \text{pH} + 0.098 \text{ V}$ . The polarization curves of the HER and OER were  $iR$ -corrected. The Tafel slopes were calculated according to the Tafel equation:  $\eta = b \log j + a$ , where  $\eta$  is the overpotential,  $b$  is the Tafel slope,  $j$  is the current density and  $a$  is the Tafel intercept relative to the exchange current density  $j_0$ . Electrochemical impedance spectroscopy (EIS) measurements were carried out in the frequency range of  $10^5$  to  $0.01 \text{ Hz}$  with AC amplitude of  $10 \text{ mV}$ . The double layer capacitance ( $C_{dl}$ ) was determined by cyclic voltammetry curves measured by scan rates of 60, 70, 80, 90 and  $100 \text{ mV s}^{-1}$ . Notably, the generated  $\text{H}_2$  and  $\text{O}_2$  gases during overall water splitting were quantitatively collected by the water drainage method.

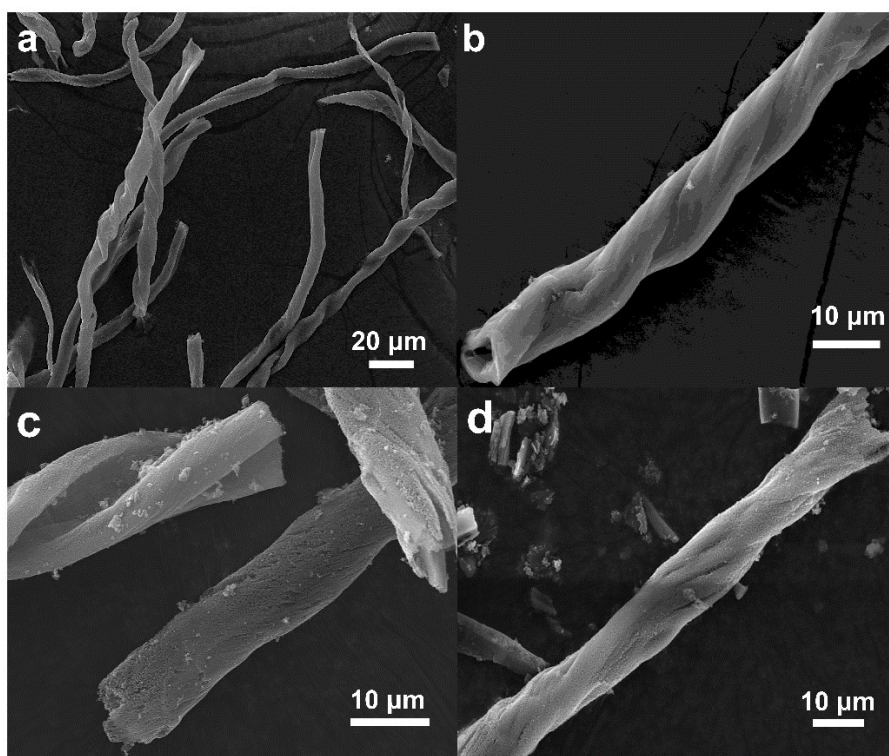


**Fig. S1.** SEM images of (a, b) BCFs and (c, d) Co/N-BCFs.

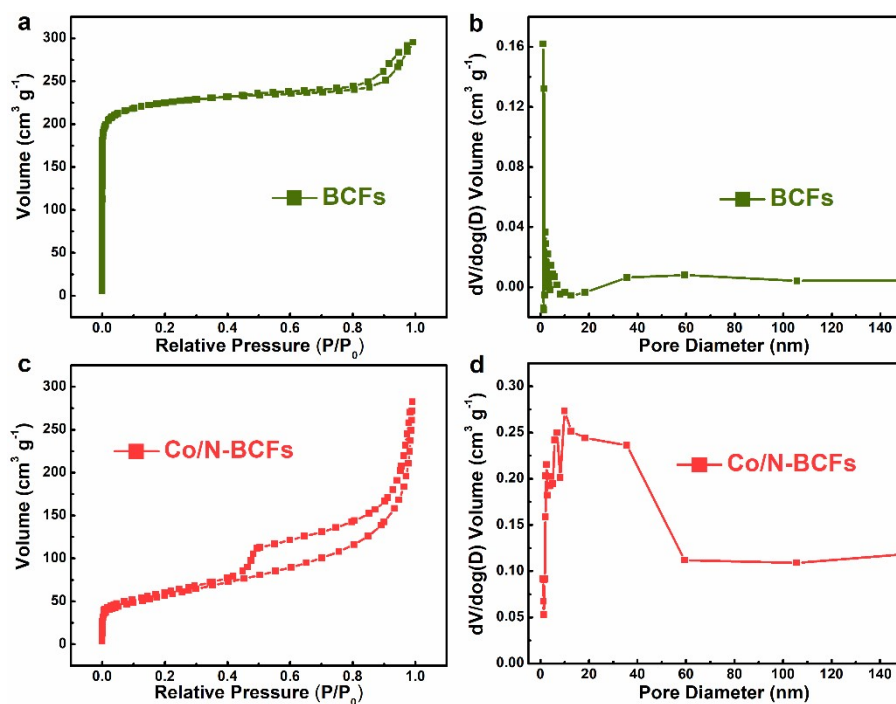


**Fig. S2.** (a, c) N<sub>2</sub> sorption isotherms and (b, d) pore size distributions of BCFs and Co/N-BCFs.

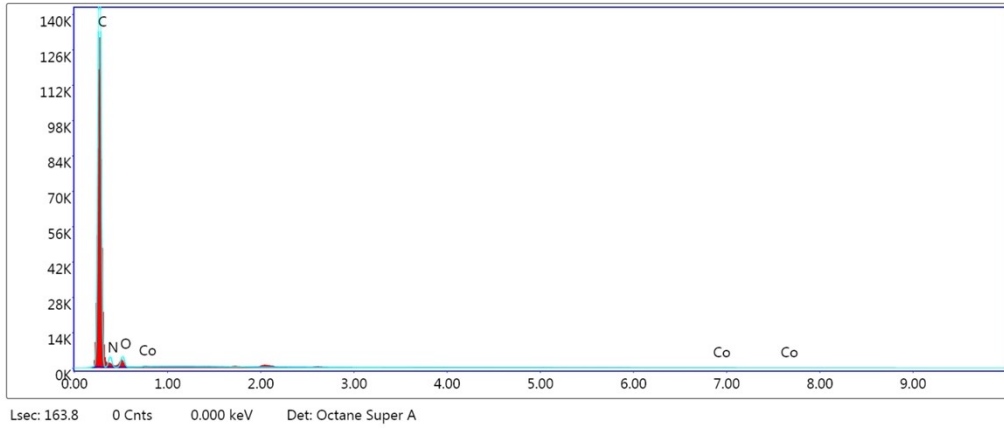


**Fig. S3.** SEM-EDS spectrum of Co/N-BCFs.

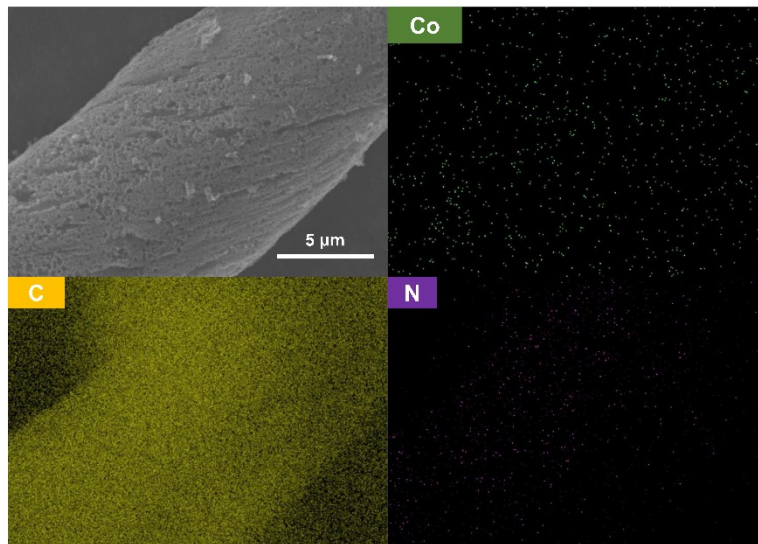


**Fig. S4.** SEM and corresponding elemental mapping images of Co/N-BCFs.

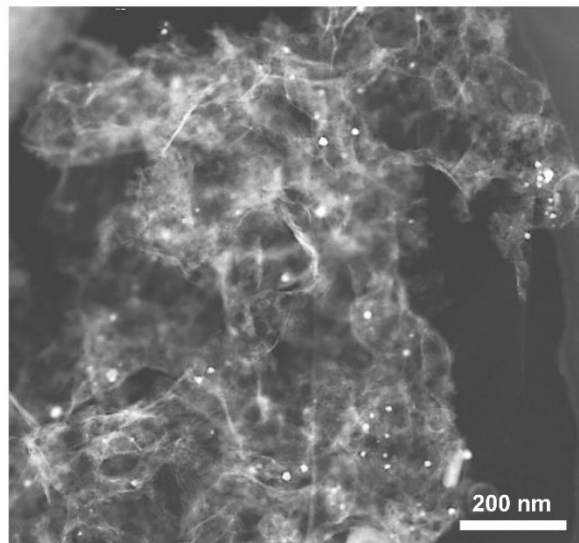


**Fig. S5.** HAADF-TEM image of Co/N-BCFs.

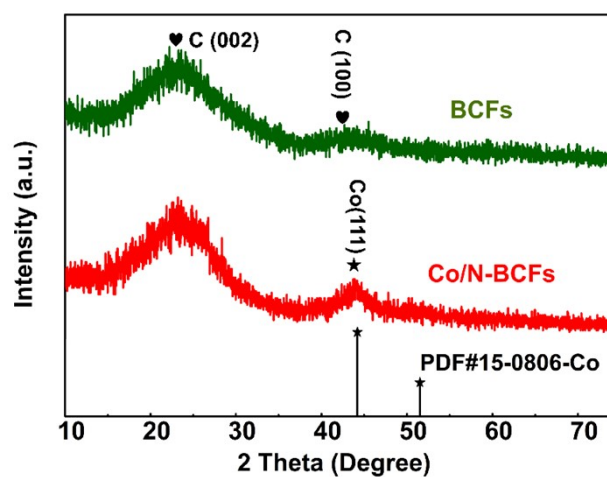


Fig. S6. XRD spectra of BCFs and Co/N-BCFs.

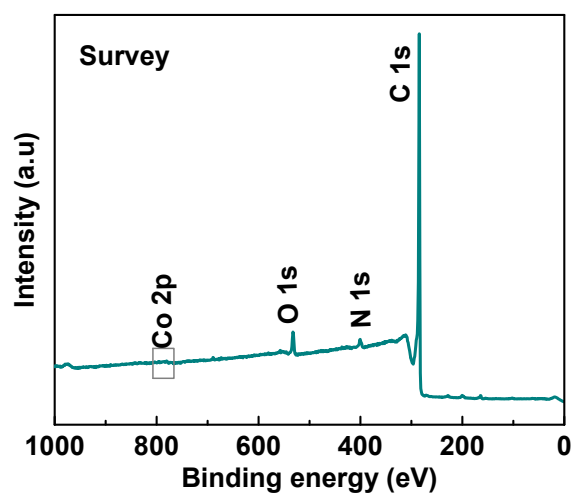


Fig. S7. Survey XPS of Co/N-BCFs.

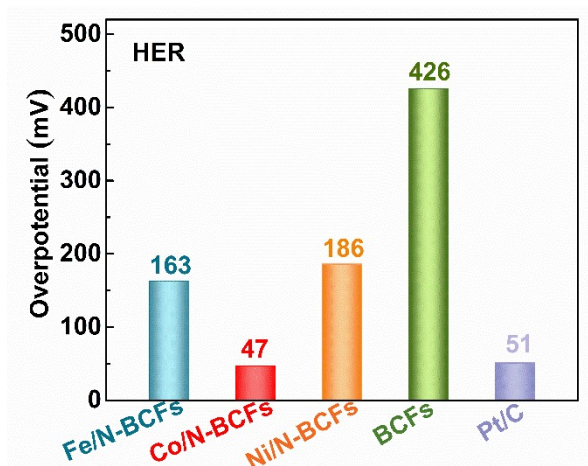


Fig. S8. HER corresponding overpotentials at 10 mA cm<sup>-2</sup> for Co/N-BCFs, Fe/N-BCFs, Ni/N-BCFs, BCFs and Pt/C.

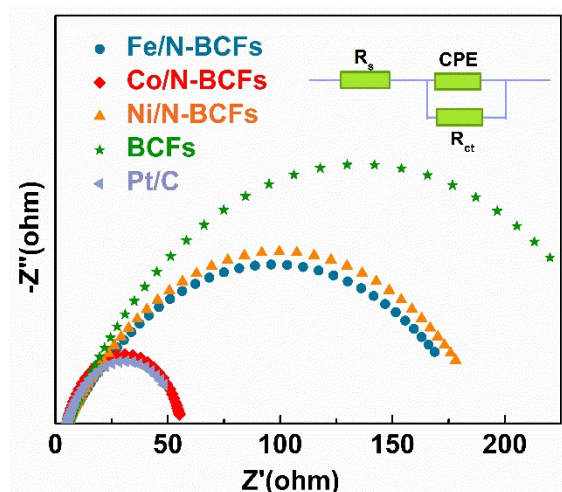


Fig. S9. Nyquist plots of Co/N-BCFs, Fe/N-BCFs, Ni/N-BCFs, BCFs and Pt/C with the fitting curves for HER.

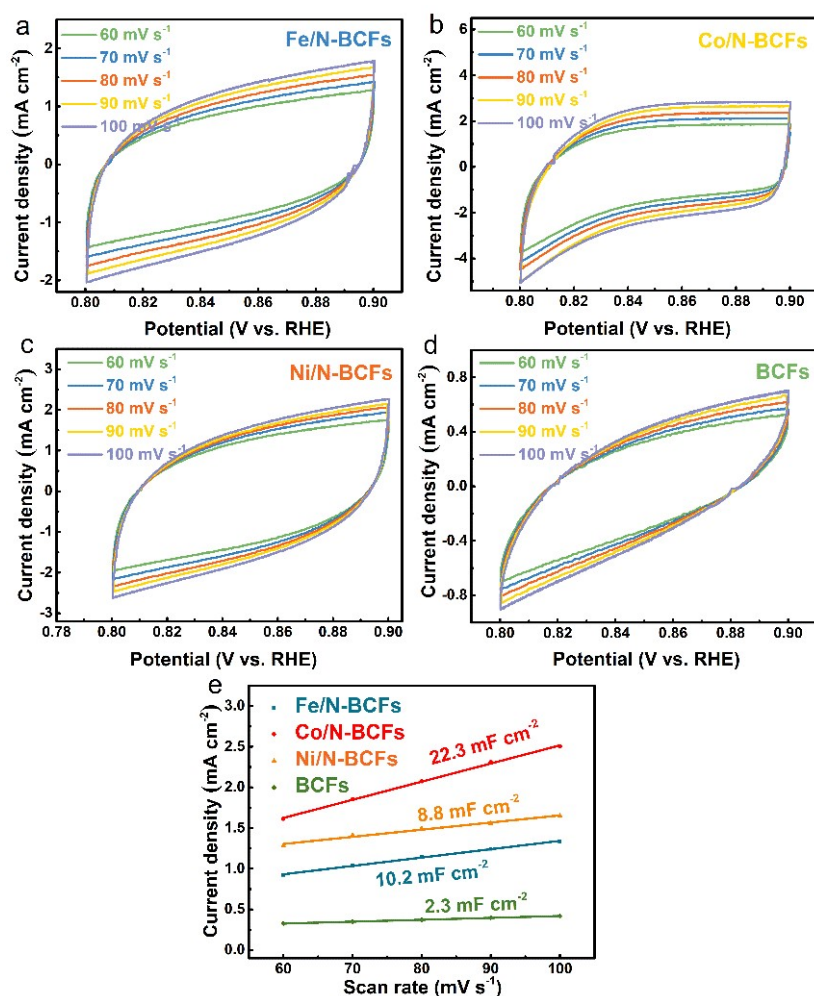
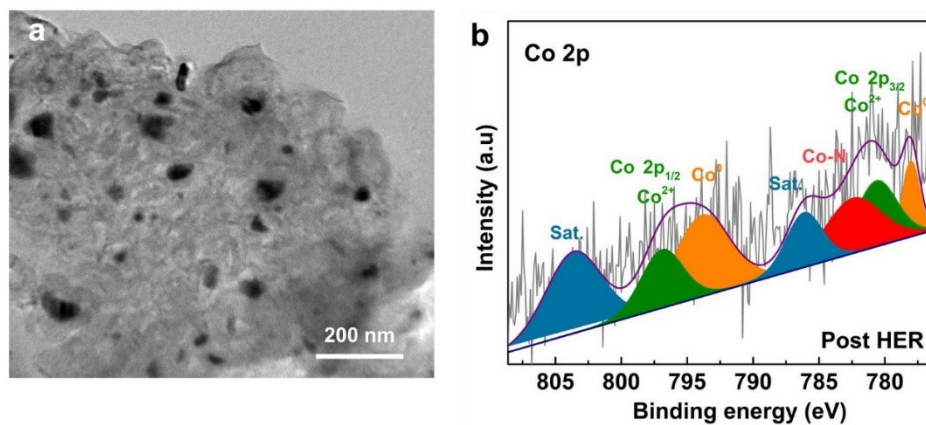
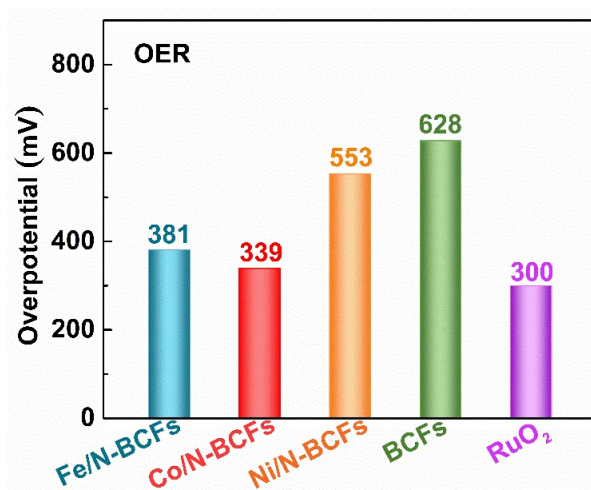


Fig. S10. Cyclic voltammograms of (a) Co/N-BCFs, (b) Fe/N-BCFs, (c) Ni/N-BCFs, and (d) BCFs in the region of 0.8 - 0.9 V (vs. RHE) at different scan rates, (e) Double-layer capacitance ( $C_{dl}$ ) of Co/N-BCFs, Fe/N-BCFs, Ni/N-BCFs and BCFs.



**Fig. S11.** (a) TEM image of Co/N-BCFs and (b) High-resolution XPS spectrum of Co 2p after HER electrolysis.



**Fig. S12.** OER corresponding overpotentials at 10 mA cm<sup>-2</sup> for Co/N-BCFs, Fe/N-BCFs, Ni/N-BCFs, BCFs and RuO<sub>2</sub>.

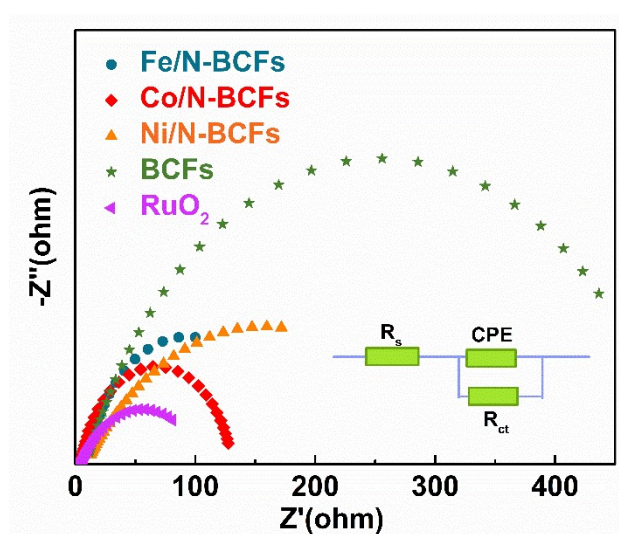


**Fig. S13.** Nyquist plots of Co/N-BCFs, Fe/N-BCFs, Ni/N-BCFs, BCFs and Pt/C with the fitting curves for OER.

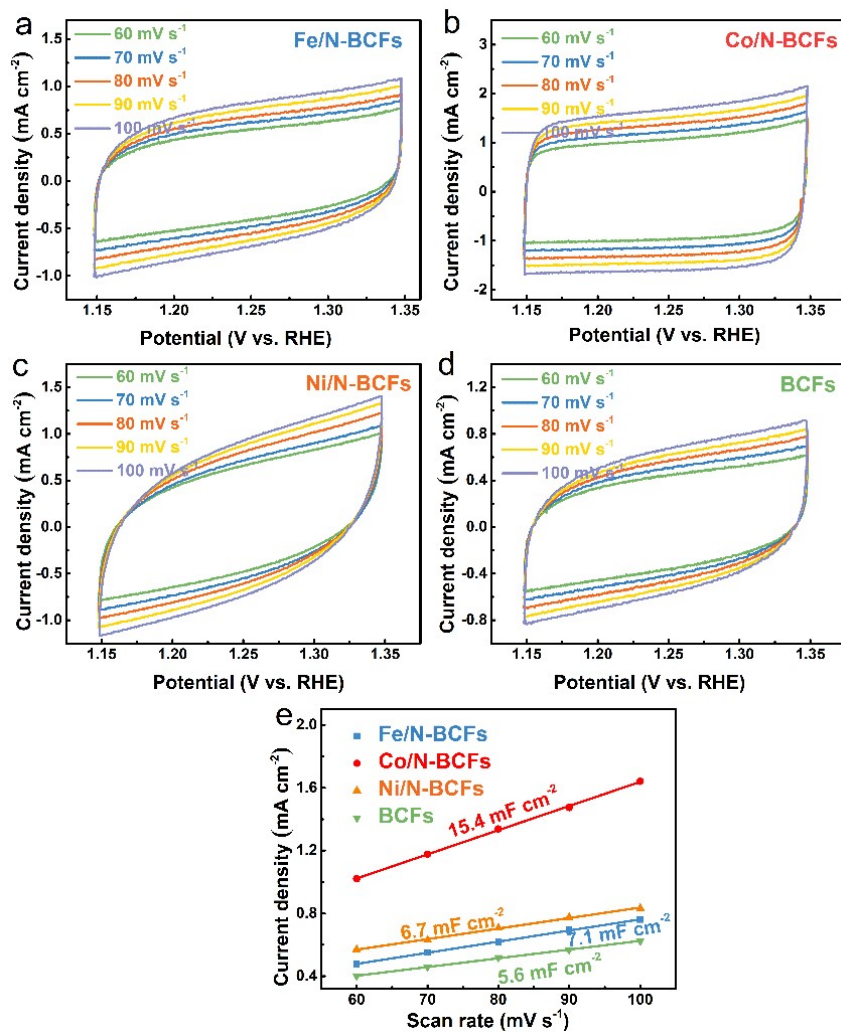


**Fig. S14.** Cyclic voltammograms of (a) Co/N-BCFs, (b) Fe/N-BCFs, (c) Ni/N-BCFs, and (d) BCFs in the region of 1.15 – 1.35 V (vs. RHE) at different scan rates, (e) Double-layer capacitance ( $C_{dl}$ ) of Co/N-BCFs, Fe/N-BCFs, Ni/N-BCFs and BCFs.

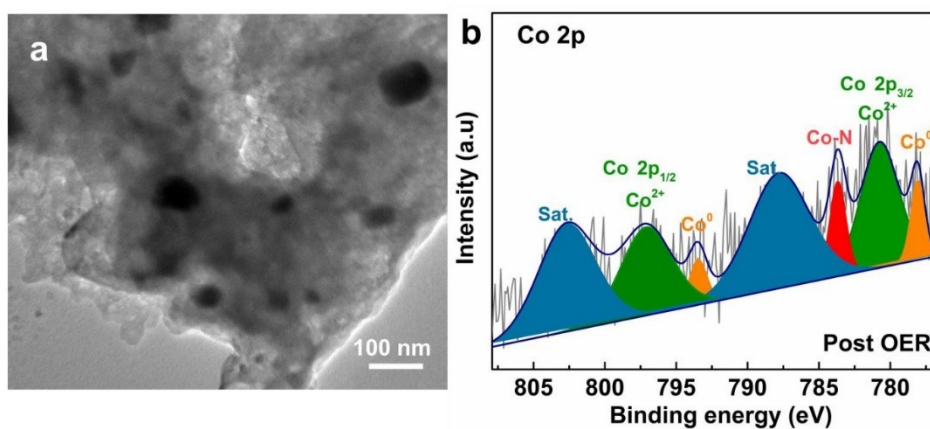


**Fig. S15.** (a) TEM image of Co/N-BCFs and (b) High-resolution XPS spectrum of Co 2p after OER electrolysis.



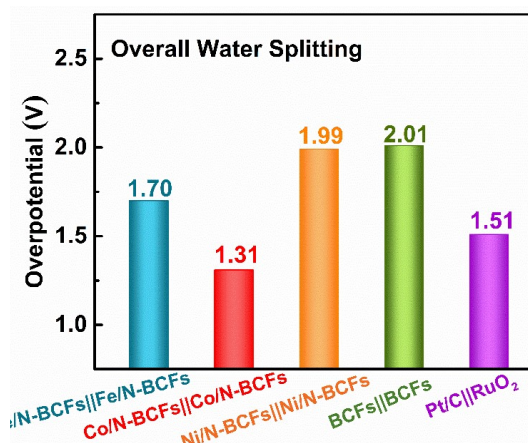


**Fig. S16.** The overpotentials at 10 mA cm<sup>-2</sup> for Co/N-BCFs||Co/N-BCFs, Fe/N-BCFs||Fe/N-BCFs, Ni/N-BCFs||Ni/N-BCFs, BCFs||BCFs and Pt/C||RuO<sub>2</sub> in overall water splitting.

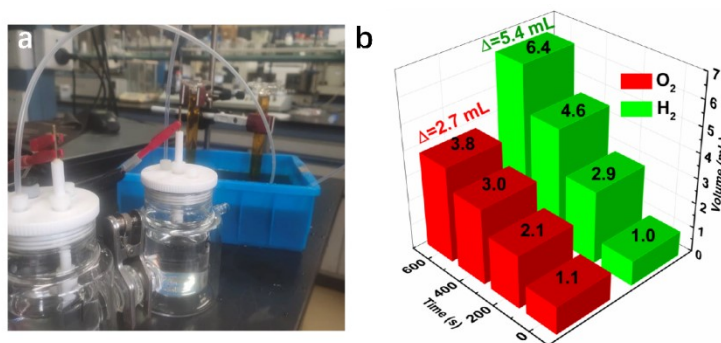


**Fig. S17.** (a) Faradic efficiency measurement device based on water splitting; (b) The variations of amount of H<sub>2</sub> and O<sub>2</sub> with time.

**Table S1.** Comparison of HER performance of Co/N-BCFs and metal-nitrogen doped carbon-based catalysts in literatures.

Electrocatalysts	Electrolytes	E <sub>j10</sub> (mV vs. RHE)	References
<b>Co/N-BCFs</b>	<b>1.0M KOH</b>	<b>47</b>	<b>This work</b>
CoFe <sub>2</sub> O <sub>4</sub> /SWNTs	1.0M KOH	263	ACS Appl. Energy Mater. 2019, 2, 1026–1032
Co@Co <sub>3</sub> O <sub>4</sub> -NC	1.0M KOH	221	J. Mater. Chem. A, 2017,5, 9533-9536
Co <sub>3</sub> Fe <sub>7</sub> @NCNTFs	1.0M KOH	197	Chem. Asian J,2020.7, 1728-1735
Co-SCN/RGO	1.0M KOH	150	ACS Sustainable Chem. Eng, 2019, 7, 15373-15384
C@Mo <sub>2</sub> C/Co	1.0M KOH	146	Int J. Hydrogen Energy, 45 (2020) 22629-22637
Co-CeO <sub>2</sub> @CNF	1.0M KOH	92	Materials 2020, 13, 856
CoN-400/CC	1.0M KOH	97	Electrochimica Acta, 273 (2018) 229-238
N, Co-CNTs	1.0M KOH	151	Appl. Catal. B-Environ, 2021, 283, 119643
Fe-Ni <sub>3</sub> C-2%	1.0M KOH	292	Angew. Chem. Int. Ed. 2017, 56, 12566–12570
Co <sub>6</sub> W <sub>6</sub> C@NC	1.0M KOH	59	Small, 2020, 16, 1907556

**Table S2.** Comparison of OER performance of Co/N-BCFs samples and metal-nitrogen doped carbon-based catalysts in literatures.

Electrocatalysts	Electrolytes	$E_{j10}$ (mV vs. RHE)	References
<b>Co/N-BCFs</b>	<b>1.0M KOH</b>	<b>339</b>	<b>This work</b>
CoFe <sub>2</sub> O <sub>4</sub> /SWNTs	1.0M KOH	310	ACS Appl. Energy Mater. 2019, 2, 1026–1032
N, Co-CNTs	1.0M KOH	308	Appl. Catal. B-Environ, 2021, 283, 119643
Fe-Ni <sub>3</sub> C-2%	1.0M KOH	275	Angew. Chem. Int. Ed. 2017, 56, 12566–12570
CoMoN <sub>x</sub> -500 NSAs/NF	1.0M KOH	231	Adv. Sci. 2020, 7, 1901833
Co <sub>6</sub> W <sub>6</sub> C@NC	1.0M KOH	286	Small, 2020, 16, 1907556
Co <sub>9</sub> S <sub>8</sub> /NC	0.1M KOH	400	RSC Adv., 7 (2017) 19181-19188.
RuNi-NCNFs	1.0M KOH	290	ACS Sustainable Chem. Eng., 6 (2018) 1527-1531.
Co-N-C	0.1M KOH	250	ACS Appl. Mater. Interfaces, 2019, 11, 39809–39819
Co/β Mo <sub>2</sub> C@NCNTs	1.0M KOH	356	Angew. Chem. Int. Ed., 2019, 58, 4923-
Co/CNFs	1.0M KOH	320	Energy Environ. Sci. 2016, 9 (2), 478

**Table S3** Comparison of water splitting performances of Co/N-BCFs samples and metal-nitrogen doped carbon-based catalysts in literatures.

Electrocatalysts	Electrolyt	$E_{j10}$ (V)	References
<b>Co/N-BCFs</b>	<b>1.0M KOH</b>	<b>1.31</b>	<b>This work</b>
CoFe <sub>2</sub> O <sub>4</sub> /SWNTs	1.0M KOH	1.72	ACS Appl. Energy Mater. 2019, 2, 1026–1032
Co@Co <sub>3</sub> O <sub>4</sub> -NC	1.0M KOH	1.75	J. Mater. Chem. A, 2017,5, 9533-9536
Co <sub>3</sub> Fe <sub>7</sub> @NCNTFs	1.0M KOH	1.64	Chem. Asian J, 2020,7, 1728-1735
Co-SCN/RGO	1.0M KOH	1.63	ACS Sustainable Chem. Eng. 2019, 7, 15373-15384
C@Mo <sub>2</sub> C/Co	1.0M KOH	1.67	Int J. Hydrogen Energ, 45 (2020) 22629-22637
CoN-400/CC	1 M KOH	1.58	Electrochimica Acta, 273 (2018) 229-238
N, Co-CNTs	1.0M KOH	1.69	Appl. Catal. B-Environ, 2021, 283, 119643
Fe-Ni <sub>3</sub> C-2%	1.0M KOH	1.56	Angew. Chem. Int. Ed. 2015, 54, 6251–6254
Co <sub>6</sub> W <sub>6</sub> C@NC	1.0M KOH	1.59	Small, 2020, 16, 1907556
CoMoN <sub>x</sub> -500 NSAs/NF	1.0M KOH	1.55	Chem. Eng. J, 2021, 411, 128433

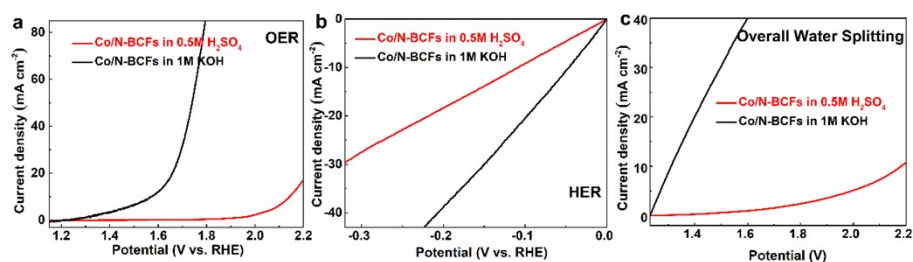


**Fig. S18** (a) OER polarization curves, (b) HER polarization curves and (c) Polarization curves for overall water-splitting of Co/N-BCFs in acidic medium.